CHARACTERISTIC DISTRIBUTION AND SCALE INTERACTION OF TURBULENCE IN A BOUNDARY LAYER

Patrick Bechlars[1], & Richard D. Sandberg [1]
[1]*Aerodynamics and Flight Mechanics Group, University of Southampton, Southampton, UK*

Abstract This work revisits the concept of turbulent boundary layers from a novel perspective on scale transfer. Turbulence production and dissipation together with the energy budgets are analyzed in the velocity gradient invariant phase space. In combination with filtering, the mechanism of scale coupling is investigated and illustrated for different characteristic flow topologies. The understanding of the scale coupling is important to model turbulence. Turbulence models describe the complex interaction of the scales of motion in a simplified form. The essential task of turbulence modeling is to capture the coupling of the modeled and unmodeled scales as well as the evolution of the modeled scales within the unmodeled flow. This work characterizes the scale coupling by focusing on the interfaces between modeled and unmodeled flow such as production and dissipation. The mechanisms that govern the evolution of the modeled quantities are investigated for their core properties and universal features. Direct numerical simulation (DNS) is carried out to obtain data of a compressible zero pressure-gradient flat plate turbulent boundary layer flow. This flow topology allows to unveil the effect of a wall on the coupling of scales and evolution of turbulence.

INTRODUCTION

DNS of a zero pressure gradient compressible pressure gradient flat plate turbulent boundary layer flow at a Mach number of $M = 0.5$ ([1]) is conducted to investigate in detail the turbulence in wall-bounded shear layer without the influence of mean pressure gradients or obstacles in the flow. The nature of turbulence rapidly changes in the inhomogeneous wall-normal direction. The DNS flow data are sampled in a physical domain for a momentum thickness Reynolds number range of $Re_\theta \approx 670 - 2300$. The Navier-Stokes equations are discretized with standard finite differences of fourth-order accuracy in the streamwise and wall-normal directions and by a decomposition in Fourier space in the homogeneous periodic spanwise direction (see [3]). The time is discretized using a five-step fourth-order accurate Runge-Kutta scheme. The resulting grid of $7200 \times 260 \times 386$ collocation points has a resolution in wall-normal units of $\Delta x^+ < 5.2$, $y^+|_1 < 0.7$ and $\Delta z^+ < 4.2$.

To apply turbulence models in a flow which is governed by the Navier-Stokes equations, the terms of the latter have to be decomposed into their unmodeled and modeled contribution. The resulting energy balances are

$$\frac{\partial \bar{\rho}\widetilde{e}}{\partial t} + \nabla \cdot \left(\tilde{\vec{u}}\bar{\rho}\tilde{e}\right) = \nabla \cdot \bar{\vec{q}} + \nabla \cdot c_{\text{e-u}} - \bar{p}\left(\nabla \cdot \tilde{\vec{u}}\right) + \left\langle \bar{\tau}, \nabla\tilde{\vec{u}} \right\rangle_F - \vartheta + \varepsilon, \tag{1}$$

$$\frac{\partial \bar{\rho}\tilde{e}_{\text{f}}}{\partial t} + \nabla \cdot \left(\bar{\rho}\tilde{\vec{u}}\tilde{e}_{\text{f}}\right) = \nabla \cdot \left(\sigma \cdot \tilde{\vec{u}}\right) - \nabla \cdot \left(\tilde{\vec{u}}\bar{p}\right) + \nabla \cdot \left(\bar{\tau} \cdot \tilde{\vec{u}}\right) + \bar{p}\left(\nabla \cdot \tilde{\vec{u}}\right) - \left\langle \bar{\tau}, \nabla\tilde{\vec{u}} \right\rangle_F - \left\langle \sigma, \nabla\tilde{\vec{u}} \right\rangle_F, \tag{2}$$

$$\frac{\partial \bar{\rho}k}{\partial t} + \nabla \cdot \left(\tilde{\vec{u}}\bar{\rho}k\right) = \nabla \cdot c_{\tau\text{-u}} - \nabla \cdot \chi - \nabla \cdot c_{\text{u-p}} + \left\langle \sigma, \nabla\tilde{\vec{u}} \right\rangle_F + \vartheta - \varepsilon. \tag{3}$$

The terms indicated with tilde or bar are the unmodeled contributions, whereas the remaining ones need to be captured by the respective turbulence model. These equations are representing the energy budgets for e.g., Reynolds averaged Navier-Stokes (RANS) or Large-Eddy Simulation (LES). Eq.(1) is the transport equation for the unmodeled internal energy $\tilde{e}$, eq.(2) is the transport equation for the unmodeled kinetic energy $\bar{e}_f$ and eq.(3) is the transport equation for the modeled kinetic energy k, which is referred to as turbulent kinetic energy or subgrid-scales energy in RANS or LES, respectively. The three different colors emphasize the terms that couple the equations and transfer energy between the respective quantities. These colored terms will be characterized in detail.

RESULTS

The averaged energy budgets (fig.1) are a first indication for the change of the mechanisms driving turbulence with wall-normal location. This variation affects the mean turbulent kinetic energy overall as well as small scales and large scales of motion separately.

Based on the *critical point concept* of [2] turbulent structures can be classified into four characteristic topologies which are defined by the respective state in invariant phase-space of the velocity gradient. For incompressible flows as well as flows with minor compressibility effects it is sufficient to consider the projection of the full invariant phase-space onto the phase-space spanned by the second and third invariant Q and R. The mean distribution of those characteristic topologies (fig.2) shows strong differences for different wall-normal locations.

The conditioning of the production with Q and R reveals which characteristic topologies are producing turbulent kinetic energy and which ones are destructing it (fig. 3). In the same way the dissipative nature of certain topologies is shown

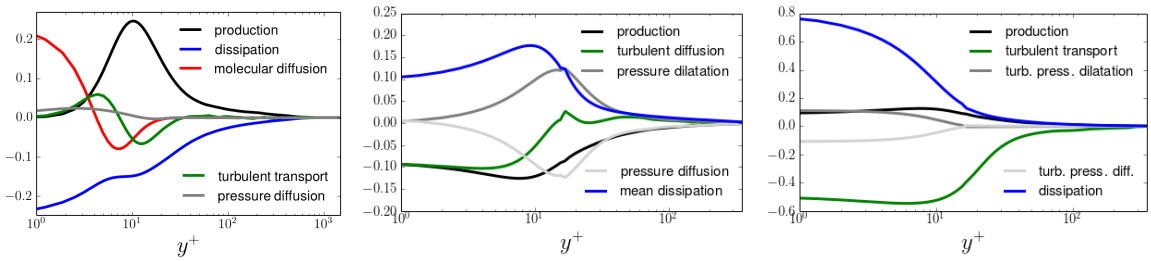

Figure 1. Turbulent kinetic energy budget (left), kinetic energy budget of the filtered velocity field with a filter width $\Delta^+ = 15$ (center), budget of the fluctuation energy w.r.t. a filter width of $\Delta^+ = 15$ (right).

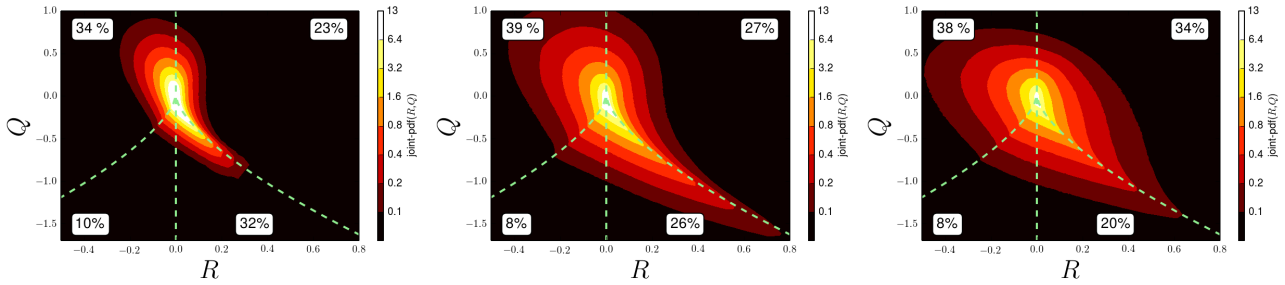

Figure 2. Joint-pdf of the 2nd and 3rd invariant Q and R of $\nabla\vec{u}$ for the outer layer (left), the log-layer (center) and the viscous sublayer (right). The dashed green lines separate four characteristic topologies ([2]) and the ratios indicate their frequency of occurrence.

in fig. 3. A significant difference of the production as well as dissipation can be seen by comparing the conditional averages for log-layer and viscous sublayer in the case of Reynolds averaged energy budgets. By comparing dissipation and production in case of filtered energy budgets with the Reynolds averaged analogue, significant differences are stated for the viscous sublayer.

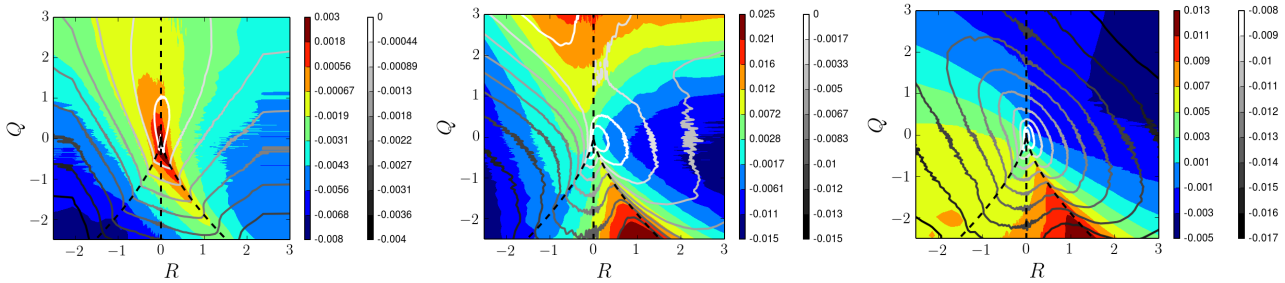

Figure 3. Dissipation (gray lines) and mean production (colored contours) in the log-layer (left) and the viscous sublayer (center;right). The plots show results for Reynolds average equations (left;center) and the filtered flow data with a filter width of $\Delta^+ \approx 15$ (right).

The presentation will summarize the important conclusions and extract the link between the scale interaction and the characteristic topologies. A clear impression of this novel perspective on scale coupling will be delivered and the role of the wall will be illustrated in detail.

References

[1] Patrick Bechlars and Richard D. Sandberg. Effects of a Wall on the Dynamics of Turbulence *Teardrops and Fingerprints*. *Proceedings of the iTi Conference in Turbulence 2014*, **VI**, to be published.

[2] Anthony E. Perry and Min S. Chong. A Description of Eddying Motions and Flow Patterns using Critical-Point Concepts. *Annual Review of Fluid Mechanics*, **19**:125–155, 1987.

[3] Richard D. Sandberg, Neil D. Sandham, and V Suponitsky. DNS of compressible pipe flow exiting into a coflow. *International Journal of Heat and Fluid Flow*, **35**:33–44, 2012.